Raman scattering from coupled plasmon-phonon modes in HgTe

M. L. Bansal, A. P. Roy, and Alka Ingale*
Nuclear Physics Division, Bhabha Atomic Research Centre, Trombay, Bombay 400 085, Maharashtra, India
(Received 16 February 1990)

An inelastic-light-scattering experiment from the (100) face of *p*-type HgTe, a zero-band-gap semiconductor, is reported. The spectral features, which involve coupling of the longitudinal phonon mode with the multicomponent plasma comprised of light electrons in the Γ_8^c conduction band and heavy holes in the Γ_8^v valence band, are analyzed by calculating $\mathrm{Im}[\epsilon^{-1}(q,\omega)]$, where $\epsilon(q,\omega)$ is the frequency- and wave-vector-dependent dielectric function of the medium. The sharp peak at 138 cm^{-1} is ascribed to "forbidden" LO-phonon scattering. The partially screened allowed LO phonon appears as a broad peak around 127 cm^{-1}, which is higher than the TO-phonon frequency ($\sim$118 cm^{-1}). The hole carriers give rise to additional features in the spectrum around 160 cm^{-1}. The results of infrared-reflectivity measurements by Grynberg *et al.* are also discussed in light of Raman data. While the ir spectra can be analyzed using $\epsilon(\omega)$, it is seen that a finite wave vector involved in the light-scattering experiment modifies the phonon-plasmon spectrum profoundly.

I. INTRODUCTION

Coupling of carriers (electrons or holes) with polar longitudinal-optical modes in doped semiconductors have been extensively investigated by an inelastic-light-scattering technique.[1,2] The macroscopic electric field associated with both of these excitations provides a strong-coupling mechanism. The frequency–wave-vector dispersion relations of the coupled modes $LO^{\mp}(q)$ can be obtained from a knowledge of the frequency- and wave-vector-dependent dielectric function $\epsilon(q,\omega)$ of the medium. Much of this work has been carried out in *n*-type GaAs.[3,4] $\epsilon(q,\omega)$ can be expressed as sum of the contributions arising from phonons ϵ_{ph}, electronic intraband transitions ϵ_e, and electronic interband transitions ϵ_{inter}. Since characteristic phonon energy is a small fraction of the electronic band gap even in narrow-band-gap semiconductors like InSb, the last term can be taken as constant in the phonon frequency range and is generally represented as $\epsilon(\infty)$. HgTe, a zero-band-gap semiconductor, provides an interesting and a rare example where electronic transition energies between the valence (Γ_8^v) and conduction (Γ_8^c) bands overlap with phonon energy[5] (Fig. 1). Consequently it cannot be simply included in $\epsilon(\infty)$. Grynberg *et al.*[5] have shown that contribution of a frequency-dependent dielectric function corresponding to the above interband transitions has to be explicitly considered in order to explain the observed infrared spectra of phonon-plasmon modes in HgTe.

In this paper we describe the results of our Raman measurements on longitudinal coupled modes in HgTe at different temperatures. We find that a finite wave vector involved in a light-scattering experiment has to be explicitly taken into account in analyzing the frequency and line shape of the coupled modes.

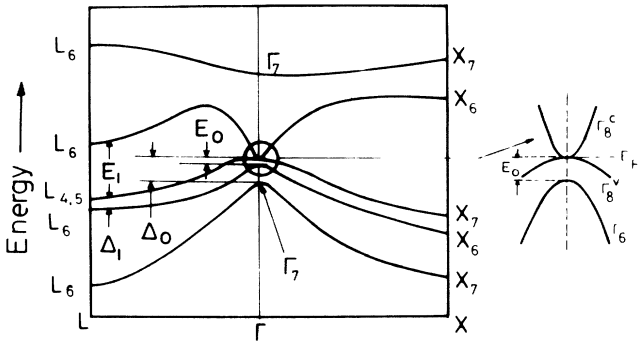

FIG. 1. Energy-band structure of HgTe. The negative energy gap $E_0 \sim 0.3$ eV, spin-orbit splitting $\Delta_0 \sim 0.9$ eV, $E_1 \sim 2.1$ eV, and $\Delta_1 \sim 0.6$ eV. The ordering of conduction and valence bands near the zone center and position of Fermi level E_F at $T=0$ K for intrinsic HgTe are indicated separately. $\Gamma_8^v \rightarrow \Gamma_8^c$ interband transition energies overlap with phonon energy.

II. EXPERIMENTAL DETAILS AND RESULTS

Thin *p*-type HgTe samples ($\sim$0.5 mm thick) were cut having the (100) face. From Hall-coefficient measurements at liquid-nitrogen (LN_2) and higher temperatures, the hole carrier concentration was inferred to be around 5×10^{17} cm^{-3}.[6] For Raman scattering experiments in the backscattering geometry, the face was mechanically polished and followed by etching in 0.01% Br_2–methanol solution. The specimen was mounted on the cold finger of a LN_2 cryostat. The Raman spectra were excited with the available lines of Ar^+ and Kr^+ lasers. The incident laser energies fall on either side of the E_1 band gap ($\sim$2.2 eV) of HgTe (Ref. 7) (Fig. 1). To avoid laser heating, the incident power was kept between 50 and 100 mW and the beam was focussed into a slit-shaped spot (size $\sim 50\ \mu m \times 1.2$ mm) on the sample surface. A computer-controlled-laser Raman spectrometer was employed for data acquisition and processing.[8] As the Raman scattered intensity from HgTe is very weak,[9] the spectra were

generally recorded without placing the Polaroid in the scattered beam.

Figures 2 and 3 show the spectra recorded from the (100) face of HgTe at various temperatures using different exciting laser lines. The low-frequency mode around 100 cm^{-1} is believed to arise from combination modes[9-11] and is not relevant to our present discussion of coupled modes. The band around 127 cm^{-1} labeled as LO^- is a coupled mode and the sharp peak at 138 cm^{-1}, seen prominently in the low-temperature spectra, is an "unscreened" LO mode. A broad feature appears around 160 cm^{-1}. Intensity at 118 cm^{-1} is also seen in some of the spectra corresponding to the position of the TO-phonon line. TO-phonon intensity is forbidden, however, in this geometry according to the usual selection rules.[12]

III. THEORY AND ANALYSIS

Light scattering by the coupled modes can arise (i) via electron density fluctuations and (ii) via the deformation potential and electro-optical mechanism.[1] The former dominates when energy of the exciting laser radiation approaches energy gaps that involve states of free carriers. In the present experiment, energy of the incident laser radiation is close to E_1 which is situated at the Brillouin-zone boundary (Fig. 1) and the free carriers are eventually located at the Γ point. Hence the charge-density mechanism is not expected to be important.[2] For the deformation potential and electro-optic mechanism, the spectral line shape for the excitation of the coupled plasmon-phonon system is given by[2]

$$L_A(q,\omega)=\left[1-\exp\left[\frac{-\hbar\omega}{kT}\right]\right]^{-1}\left[\frac{\omega_0^2-\omega^2}{\omega_{TO}^2-\omega^2}\right]^2 \times \mathrm{Im}\left[\frac{-1}{\epsilon(q,\omega)}\right], \quad (1a)$$

where ω_{TO} is the transverse-optical frequency and ω_0 is a parameter with dimensions of frequency related to the Faust-Henry coefficient.[2] A typical value of the wave vector transferred in the present light-scattering experiment is $q=q_0\sim 0.8\times 10^6$ cm^{-1}.

When incoming photon energy approaches an energy gap of the material, a q-dependent Fröhlich interaction can contribute significantly to the scattered intensity for the polar longitudinal modes. This is termed as "forbid-

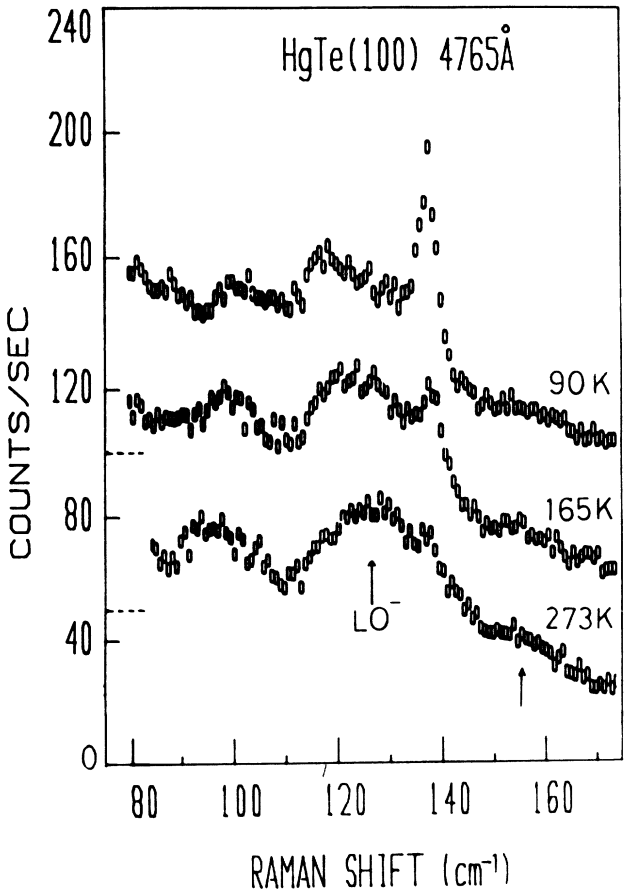

FIG. 2. Raman spectra of HgTe (100) recorded with 100 mW of 4765 Å at different temperatures. The short-dashed lines on the vertical scale indicate the zero shifts for the upper two spectra, respectively. Notice the weak feature around 160 cm^{-1}.

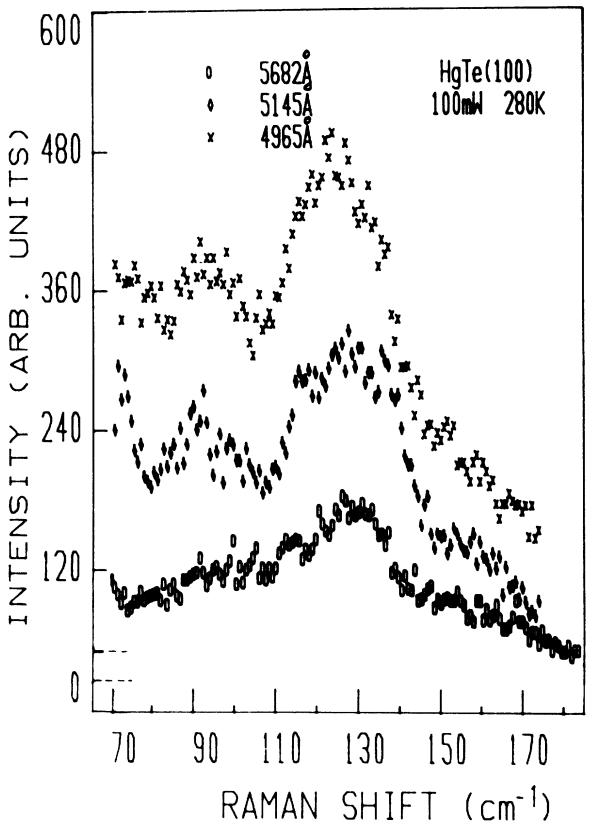

FIG. 3. Raman spectra at 280 K with different excitation wavelengths 4965, 5145, and 5682 Å. The former two correspond to energies greater than E_1 and the latter to less than the gap. The zero shifts are indicated on the vertical scale. The broad feature around 130 cm^{-1} is LO^-. Note the decrease in intensity when the exciting wavelength lies below the E_1 gap.

den" scattering in contrast to the allowed scattering mechanism discussed above. The corresponding line-shape function can be written as[2]

$$L_F(q,\omega)=\left[1-\exp\left[\frac{-\hbar\omega}{kT}\right]\right]^{-1} q^2\,\mathrm{Im}\left[\frac{-1}{\epsilon(q,\omega)}\right] . \quad (1b)$$

The various processes whose contributions to $\epsilon(q,\omega)$ need to be considered in p-type HgTe are

$$\epsilon(q,\omega)=\epsilon(\infty)+\epsilon_{\mathrm{ph}}(q,\omega)+\epsilon_e(q,\omega)+\epsilon_h(q,\omega)+\epsilon_{\mathrm{inter}}(q,\omega) . \quad (2)$$

The subscripts refer to phonons, electrons in Γ_8^c, holes in the Γ_8^v band, and $\Gamma_8^v\rightarrow\Gamma_8^c$ interband transitions (Fig. 1). The remaining interband contributions to ϵ are in effect included in $\epsilon(\infty)$. As the dispersion of the optical branch is practically zero in the neighborhood of zone center, ϵ_{ph} can be treated as q independent for q of the order of one-hundredth of the Brillouin zone. The expression used for calculating the various terms in Eq. (2) are discussed below.

We have

$$\epsilon_{\mathrm{ph}}=\frac{F\omega_{\mathrm{TO}}^2}{\omega_{\mathrm{TO}}^2-\omega^2} . \quad (3)$$

F is the oscillator strength of the TO phonon having frequency ω_{TO}. The values as determined by Grynberg *et al.*[5] from ir measurements are $F=4.7$ and $\omega_{\mathrm{TO}}\sim 118$ cm^{-1} and they are found to be almost temperature independent. We use the above values in our calculation.

The electron carrier density in HgTe at a finite temperature is contributed by (i) photoexcited carriers in the conduction band because of laser irradiation and (ii) the thermally excited carriers. Taking the absorption coefficient of HgTe as $\sim 2\times 10^5$ cm^{-1} in the visible,[13] for an incident laser beam of about 100 mW with a spot size of 50 μm $\times$ 1.2 mm, the number of photoexcited carriers is estimated to be $\sim 1\times 10^{17}$ cm^{-3}. Contribution from thermally excited carriers becomes comparable to this value at temperatures above 120 K.[14] With this electron concentration and the effective electron mass of $m_e^*=0.03m_e$ (Refs. 7 and 15) (m_e being the free-electron mass), the Thomas-Fermi screening wave vector works out to be $q_{se}\sim 0.9\times 10^6$ cm^{-1}. Since the wave vector transferred in the light-scattering experiment is also of this magnitude and the electron Fermi energy ($\sim$40 meV) is not very large compared to kT, the electronic intraband contribution to the dielectric function has to be evaluated in the Lindhard-Mermin formulation. The relevant expression is given by[2]

$$\epsilon_e(q,\omega)=\frac{4\pi(1+i\Gamma_e/\omega)[\chi_0(q,\omega+i\Gamma_e)]}{1+(i\Gamma_e/\omega)[\chi_0(q,\omega+i\Gamma_e)/\chi_0(q,0)]} , \quad (4)$$

where

$$\chi_0=\frac{1}{2\pi^3}\left[\frac{e^2}{q^2}\right]\int d^3k\, f(k,T)\left[\frac{1}{(\hbar^2q^2/m_e^*+2\hbar^2qk/m_e^*-2\hbar\omega-i2\hbar\Gamma_e)}+\frac{1}{(\hbar^2q^2/m_e^*-2\hbar^2qk/m_e^*+2\hbar\omega+i2\hbar\Gamma_e)}\right] . \quad (5)$$

TABLE I. Parameters used in the calculation of $\epsilon(q,\omega)$ and Raman line shapes at $T=165$ K for HgTe.

F:	Oscillator strength of the TO phonon	4.7[a]
ω_{TO}:	TO-phonon frequency	118 cm^{-1} [a]
ω_0:	Parameter related to Faust-Henry coefficient	50 cm^{-1}
α:	Absorption coefficient for visible radiation $\sim$5000 Å	2×10^5 cm^{-1} [b]
n_e:	Electron carrier concentration	2×10^{17} cm^{-3}
m_e^*/m_e:	Electron effective mass in Γ_8^c band in units of free-electron mass	0.03[c]
Γ_e:	Electron damping parameter	12 cm^{-1} [a]
n_h:	Hole carrier concentration	5×10^{17} cm^{-3}
m_h/m_e:	Hole effective mass in Γ_8^v band in units of free-electron mass	0.4[c]
Γ_h:	Hole damping parameter	50 cm^{-1}
$\epsilon(\infty)$:	Dielectric constant at frequencies large compare to $\Gamma_8^v\rightarrow\Gamma_8^c$ interband transition energies	10[a]
q_0:	Wave-vector transfer in the light-scattering experiment	8×10^5 cm^{-1}

[a] Reference 5.
[b] Reference 13.
[c] References 7 and 15.

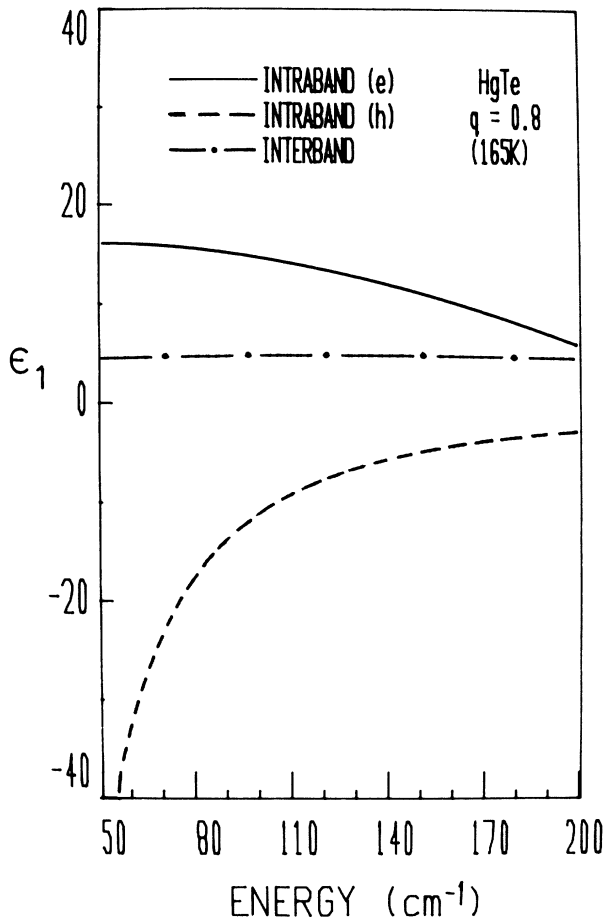

FIG. 4. Contributions to real part ϵ_1 of the dielectric constant due to intraband and interband scattering processes in the vicinity of phonon energy. The results presented here are for average q ($=0.8\times10^6$ cm^{-1}) involved in the light-scattering experiments.

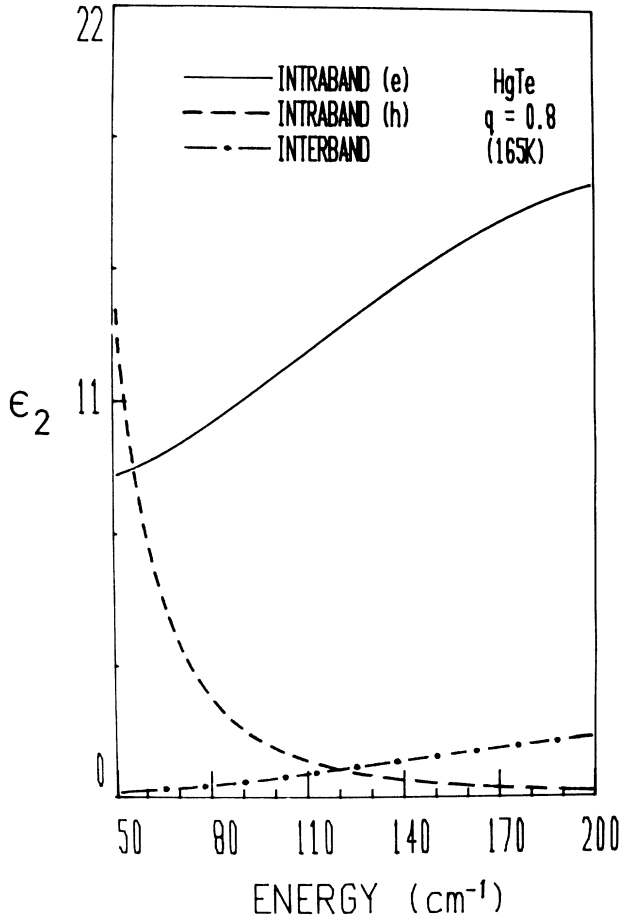

FIG. 5. Contributions to imaginary part ϵ_2 of the dielectric constant due to intraband and interband scattering processes in the vicinity of phonon energy. The results presented here are for average q ($=0.8\times10^6$ cm^{-1}) involved in the light-scattering experiments.

The calculated curves using the parameters given in Table I are shown in Figs. 4 and 5.

The hole carriers in p-type HgTe are contributed by the Γ_8^v band. Given a carrier density of $n_h\sim5\times10^{17}$ cm^{-3} (Ref. 6) and hole mass $m_h=0.4m_e$,[14] the Thomas-Fermi screening wave vector $q_{sh}\sim4\times10^6$ cm^{-1}. Thus for the hole plasma, the condition $q<q_{sh}$ holds. However, since $qv_{fh}\sim\hbar\omega$, where v_{fh} is the hole Fermi velocity, we use the hydrodynamic model to calculate $\epsilon_h(q,\omega)$[2]:

$$\epsilon_h(q,\omega)=\frac{-\epsilon(\infty)\omega_p^2}{[\omega^2-(\frac{3}{5})q^2v_{fh}^2]+i\Gamma_h}\ , \tag{6}$$

where $\omega_p=4\pi ne^2/\epsilon(\infty)m_h$, and Γ_h is hole-plasma damping parameter. The imaginary and real parts of ϵ_h are shown in Figs. 4 and 5.

The contribution to the imaginary part of the dielectric function arising from interband transitions between the heavy-hole valence band Γ_8^v and the electron conduction band Γ_8^c (Fig. 1) is given by[16]

$$\epsilon''_{\text{inter}}=\frac{-e^2}{\pi^2q^2}\int d^3k\ |\langle\mathbf{k}+\mathbf{q},c|e^{-i\mathbf{q}\cdot\mathbf{r}}|\mathbf{k},v\rangle|^2(f_c-f_v)\delta(E_c(\mathbf{k}+\mathbf{q})-E_v(\mathbf{k})-\hbar\omega)\ , \tag{7}$$

f_c and f_v being Fermi-Dirac distribution functions given by

$$f_c=\{1+\exp[(E-E_F)/kT]\}^{-1}$$

and

$$f_v=\{1+\exp[(E_F-E)/kT]\}^{-1}\ .$$

The Fermi energy for the p-type HgTe is calculated in the parabolic-band approximation with $m_e^*=0.03m_e$ and $m_h=0.4m_e$. The lower valence band Γ_6^v is ignored for

this calculation at subambient temperature as it is ~300 meV away from the upper heavy-hole valence band Γ_8^v and the exact carrier concentration is not known. Using

$$n_e = \frac{(2m_e^* kT)^{3/2}}{2\pi^2\hbar^3} \int_0^\infty E^{1/2} f_c(E)\, dE \ ,$$

$$n_h = \frac{(2m_h kT)^{3/2}}{2\pi^2\hbar^3} \int_{-\infty}^0 (-E)^{1/2} f_v(E)\, dE \ .$$

The integration is performed numerically over a range of E_F values. Of these the E_F value that results in correct hole concentration at a given temperature is used for calculating interband contribution to the dielectric constant. It may be mentioned that the situation is quite complex here owing to the presence of trapped electrons on the vacant Hg sites. However, because of large concentration of holes ($\sim 5\times 10^{17}$ cm^{-3}) which remains more or less temperature independent, it is possible to obtain an estimate of E_F.

The real part of $\epsilon(q,\omega)$ is obtained by Kramers-Kronig inversion of the imaginary part. These are plotted in Figs. 4 and 5.

As the refractive index of the crystal is complex for the laser wavelength employed in this experiment, the effect of absorption on the line-shape function [Eq. (1)] has to be taken into account. The absorption coefficient $\alpha \sim 0.2\times 10^6$ cm^{-1}; it contributes a spread to the mean wave vector $q_0 \sim 0.8\times 10^6$ cm^{-1}. Equations (1a) and (1b) are integrated to obtain the Raman line-shape function in backscattering geometry as follows:[2]

$$\langle L(\omega)\rangle_{q=q_0} = \int_{-\infty}^{+\infty} \frac{L(q,\omega)}{(q-q_0)^2+(2\alpha)^2}\, dq \ . \tag{8}$$

The line-shape function $L_A(\omega)$ calculated using Eq. (8) is shown in Fig. 6. By comparing with the experimental data Figs. 2 and 3, we find that the LO$^-$ mode (~127 cm^{-1}) lies above ω_{TO}. This feature can be related to incomplete screening of the longitudinal-optic phonon mode by the electron plasma since the phonon wave vector q_0 ($\sim 0.8\times 10^6$ cm^{-1}) is of similar magnitude as the screening wave vector q_{se} ($\sim 0.9\times 10^6$ cm^{-1}). The hole-plasma term only modifies the line shape and contributes to the wing at higher frequencies. It is important to point out here that even though electron concentration increases with increasing temperature (1×10^{17} cm^{-3} at 120 K to 3×10^{17} cm^{-3} at 250 K),[14] the position of the LO$^-$ peak does not shift appreciably. This is because the electron plasma screening wave vector q_{se} increases by only 20% over the above range of concentration and the corresponding shift in LO$^-$ is less than 3%. The above prediction is in agreement with our experimental observation of the behavior of LO$^-$ as a function of temperature. It is relevant to mention here that in the Raman spectra from the (111) face of HgTe, Amirtharaj *et al.*[17] observe a broad feature around 133 cm^{-1} which they ascribe to a screened LO phonon. For the upper plasmon branch, calculation indicates that LO$^+$ (>200 cm^{-1}) should increase rapidly with increasing n_e but it gets overdamped because of large contribution of Im(ϵ_e) (Fig. 5). Experimentally, we also do not observe any clear evidence of the LO$^+$ mode.

We next discuss the origin of the sharp peak which appears at ~138 cm^{-1} and is particularly prominent in the low-temperature spectra (Fig. 2). The intensity of this line shows a strong resonance behavior when energy of the exciting laser radiation is close to the E_1 energy-band gap. Further, intensity in the off-diagonal geometry is only 10% of that in the diagonal geometry. Thus, the origin of this mode can be ascribed to "forbidden" q-dependent LO scattering. The resonance behavior of this mode has been discussed in detail in our earlier paper.[9] It may be noted here that intensity variation of the coupled mode spectra as a function of the exciting laser wavelength (Fig. 3) follows qualitatively the behavior exhibited by the TO mode.[9]

The line-shape function $L_F(q,\omega)$ for the forbidden scattering process can be calculated using Eq. (1b) and q integration can be performed as in Eq. (8). In Fröhlich interaction, excitations with large wave vectors dominate in the scattering process. For these relatively large q values, the electric field associated with the LO mode is

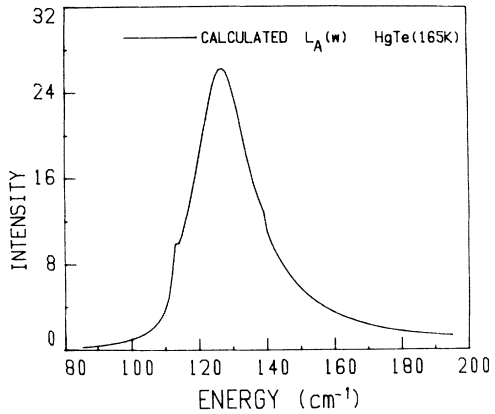

FIG. 6. The spectral line shape for the allowed light scattering from phonon-plasmon coupled system calculated using Eq. (1a) with parameters given in Table I. The experimentally observed feature at ~95 cm^{-1} (Figs. 2 and 3) can be reproduced by including an additional oscillator (Refs. 5 and 10).

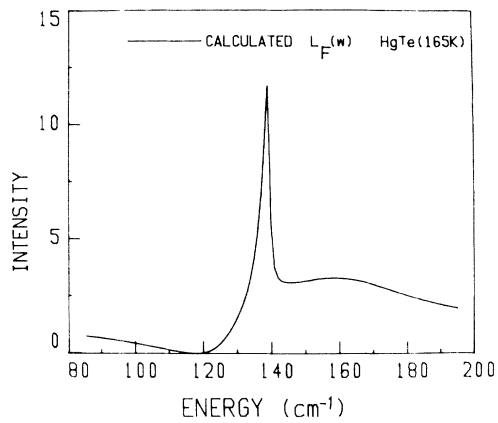

FIG. 7. The spectral line shape for the "forbidden" light scattering from phonon-plasmon coupled systems calculated using Eq. (1b) with parameters given in Table I.

not effectively screened by the carriers and ϵ_{inter} also becomes negligible. The result of the calculation is presented in Fig. 7. A sharp peak appears at 139 cm^{-1} and a broad hump at 160 cm^{-1} which is contributed by the hole plasma. These features are in excellent qualitative agreement with the observed spectra (Figs. 2 and 3).

It is interesting to point out here that in ir experiments on *n*-type HgTe, Grynberg *et al.*[5] observe the ω_{LO} frequency at 132 cm^{-1} in the absence of carriers at 8 K. In this case, q can be taken as zero. Consequently, Eq. (2) takes the form

$$\epsilon(\omega)=\epsilon(\omega)+\epsilon_{\text{ph}}(\omega)+\epsilon_{\text{inter}}(\omega) .$$

$\epsilon_{\text{inter}}(\omega)$ has large contribution for $q=0$ (Ref. 5) and the peak in $\text{Im}(1/\epsilon)$ now occurs at 132 cm^{-1}. This explains why the "unscreened" LO-phonon mode manifests at different frequencies in Raman and ir experiments. It may be emphasized here that we do not expect to see the "allowed" unscreened LO phonon in Raman scattering experiments because of the presence of photoexcited carriers which screen the mode even at the lowest temperature.[10,18] In most other semiconductors, however, the observed unscreened LO peak is attributed to the allowed LO scattering from the depletion layer.

Peak intensity of the forbidden LO mode at 138 cm^{-1} is seen to decrease with increasing temperature (Fig. 2). Excitonic contribution to intensity of the forbidden LO mode near resonance at the E_1 gap can be expected to be large at low temperatures. As the exciton band broadens rapidly with increasing temperature, its contribution to forbidden scattering becomes progressively less.

Some of the spectra shown in Fig. 2 indicate the presence of intensity around 118 cm^{-1} which corresponds to TO-phonon frequency. From selection rule considerations, TO ($q\rightarrow 0$) is forbidden in the backscattering experiment from the (100) face. Since the *p*-type HgTe sample has Hg vacancies, impurity-induced scattering leading to wave-vector nonconservation can give rise to finite intensity for the TO phonon.[19]

IV. CONCLUSIONS

The analysis of the results presented in the previous section brings out the interesting fact that the spectra contain features of both allowed and forbidden Raman scattering from coupled phonon-electron-hole plasma. It may be noted in this connection that most of the work reported so far in the literature relates to allowed scattering from coupled phonon-electron systems in semiconductors. An explanation is also given as to why in HgTe the "unscreened" LO phonon occurs at 132 cm^{-1} in infrared experiment and at 138 cm^{-1} in Raman experiments in terms of the interband contribution to the dielectric function $\epsilon(q,\omega)$.

ACKNOWLEDGMENTS

The authors are grateful to Professor A. K. Ramdas for providing the HgTe single crystal. They wish to thank Dr. B. A. Dasannacharya for his keen interest in this work.

---

*Present address: Laser Programme, Centre for Advanced Technology, Rajendra Nagar, Indore 452 012, Madhya Pradesh, India.

[1]M. V. Klein, in *Light Scattering in Solids I,* Vol. 8 of *Topics in Applied Physics,* edited by M. Cardona (Springer, Berlin, 1983), p. 147.

[2]G. Abstreiter, M. Cardona, and A. Pinczuk, in *Light Scattering in Solids IV,* Vol. 54 of *Topics in Applied Physics,* edited by M. Cardona and G. Guntherödt (Springer, Berlin, 1984), p. 5.

[3]A. Mooradian, in *Laser Handbook II,* edited by F. T. Arechi and E. O. Schulz-Du Bois (North-Holland, Amsterdam, 1972), p. 1309.

[4]G. Abstrieter, R. Trommer, M. Cardona, and A. Pinczuk, Solid State Commun. **30**, 703 (1979).

[5]M. Grynberg, R. Le Toullec, and M. Balkanski, Phys. Rev. B **9**, 517 (1974).

[6]D. Sahoo (private communication).

[7]R. Dornhaus and G. Nimtz, in *Narrow Gap Semiconductors,* Vol. 98 of *Springer Tracts in Modern Physics* (Springer, Berlin, 1980).

[8]A. P. Roy and M. L. Bansal, Indian J. Pure Appl. Phys. **26**, 218 (1988).

[9]Alka Ingale, M. L. Bansal, and A. P. Roy, Phys. Rev. B **40**, 12 353 (1989).

[10]Alka Ingale, Ph. D. thesis, Bombay University, 1989 (unpublished).

[11]J. Baars and F. Sorger, Solid State Commun. **10**, 875 (1972).

[12]M. Cardona, in *Light Scattering in Solids II,* Vol. 50 of *Topics in Applied Physics,* edited by M. Cardona and G. Guntherödt (Springer, Berlin, 1980), p. 19.

[13]Absorption coefficient at laser wavelength λ is given by $\alpha=(2\pi/\lambda)[\text{Im}(\epsilon^{1/2})]$. The complex dielectric constant ϵ for HgTe has been reported by L. Vina, C. Umbach, M. Cardona, and L. Vodopyanov, Phys. Rev. B **29**, 6752 (1987).

[14]R. R. Galazka, Phys. Lett. **32A**, 101 (1970).

[15]*Semiconductors: Physics of II-VI and I-VII Compounds, Semiconductors, Landolt-Börnstein New Series, Vol. III/17B,* edited by O. Madelung (Springer, Berlin, 1982), p. 239.

[16]J. G. Broerman, in *Proceedings of the 11th International Conference on the Physics of Semiconductors* (Elsevier, Amsterdam, 1972), p. 917, Vol. 2.

[17]P. M. Amirtharaj, K. K. Tiong, P. Parayanthal, and F. H. Pollak, J. Vac. Sci. Technol. **A3**, 226 (1985).

[18]The spectra at around 10 K exhibit features similar to the spectra at LN_2 temperature, indicating significantly higher electron concentration than would be expected using thermodynamic considerations.

[19]D. Olego and M. Cardona, Phys. Rev. B **24**, 7217 (1984).